Journal of Water Process Engineering 50 (2022) 103291

Contents lists available at ScienceDirect

Journal of Water Process Engineering

journal homepage: www.elsevier.com/locate/jwpe

Multi-cycle regeneration of arsenic-loaded iron-coated cork granulates for water treatment

Mariko A. Carneiro, Joana F.R. Coelho, Ariana M.A. Pintor *, Rui A.R. Boaventura, Cidália M.S. Botelho

Laboratory of Separation and Reaction Engineering – Laboratory of Catalysis and Materials (LSRE-LCM), Department of Chemical Engineering, Faculty of Engineering, University of Porto, Rua Dr. Roberto Frias, 4200-465 Porto, Portugal
ALiCE - Associate Laboratory in Chemical Engineering, Faculty of Engineering, University of Porto, Rua Dr. Roberto Frias, 4200-465 Porto, Portugal

ARTICLE INFO

Keywords:
Adsorption
Arsenate
Desorption
Modified biosorbent
Fixed-bed column

ABSTRACT

The chemical desorption of arsenic from saturated iron-coated cork granulates (ICG) and the regeneration capacity of this adsorbent for further reuse was investigated in batch and continuous modes. Different types of eluents were tested at different concentrations for evaluating their desorption capacity, and leaching of total organic carbon (TOC), iron content, and characterization by SEM/EDS were used to assess the eluents' attack on the adsorbent structure. The NaOH 0.1 M solution achieved the highest arsenic removal rate from saturated media; however, it was aggressive to the adsorbent structure, as reflected in high TOC values found in the eluate, higher iron leaching from the adsorbent, and degradation of cork cellular structure. The Elovich model fitted best ($r^2 > 0.98$) the desorption kinetics when using NaOH as eluent. The less basic solution of NaOH 0.01 M proved to be less aggressive to ICG and allowed media regeneration for at least four adsorption-desorption cycles, while remaining an arsenic adsorption capacity of 1 mg g^{-1} in both batch and continuous modes. ICG's adsorption capacity was less affected after various cycles than other adsorbents, so this material proved to be potentially applicable as an alternative green solution for arsenic removal from water. The adsorbent was also successfully applied in continuous mode to remove arsenic from real groundwater and was able to maintain arsenic concentration under 10 and 50 μg L^{-1} for 140 and 341 bed volumes, respectively. This work provided good insights on arsenic desorption from ICG and its further application in similar real scenarios.

1. Introduction

Arsenic's first guideline for drinking water was established 80 years ago (at least in the U·S) [1,2]. In 1958, the World Health Organization (WHO) published the first International Standards for Drinking Water which fixed an admissible level of arsenic at 0.2 mg L^{-1} [3]. Nevertheless, the concern about its consumption has been known for millennia, and for some time, its name was used as a synonym for poison. Much time has passed, but water contamination with arsenic is still an obstacle in many parts of the globe. And not surprisingly, the publications of academic papers about arsenic in drinking water have raised, in two decades (1992–2011), from the least to the most researched contaminant among the most frequently studied pollutants: arsenic, nitrate, fluoride, lead, and cadmium [4]. Moreover, in the last decade there was an increase of nearly 50 % in the number of Scopus-Indexed documents related to arsenic and drinking water.

Arsenic is environmentally present in both organic and inorganic species, being the inorganic forms more toxic and found in water bodies [5]. The contamination of water with arsenic can be related to natural and anthropogenic sources. It was reported [6] that >230 million people in almost 108 countries are at risk of drinking arsenic-contaminated water, being nearly half of the population affected placed in Asia. In addition, 92 % of OECD nations are affected by arsenic contamination in groundwater [6]. So, exposure to arsenic is still a major global health issue, and further deep investigation should be conducted on its effects on human health [7].

Various researchers are developing more sustainable and cost-effective technologies to limit the impacts of arsenic-polluted water, from biosensors for As detection [8] to biosorbents for As removal from

---

* Corresponding author at: Laboratory of Separation and Reaction Engineering – Laboratory of Catalysis and Materials (LSRE-LCM), Department of Chemical Engineering, Faculty of Engineering, University of Porto, Rua Dr. Roberto Frias, 4200-465 Porto, Portugal.

E-mail addresses: mariko.carneiro@fe.up.pt (M.A. Carneiro), up201905891@edu.fe.up.pt (J.F.R. Coelho), ampintor@fe.up.pt (A.M.A. Pintor), bventura@fe.up.pt (R.A.R. Boaventura), cbotelho@fe.up.pt (C.M.S. Botelho).

https://doi.org/10.1016/j.jwpe.2022.103291
Received 5 July 2022; Received in revised form 12 October 2022; Accepted 28 October 2022
Available online 15 November 2022

List of acronyms

BTC	Breakthrough curve
EBCT	Empty bed contact time
EDS	Electron dispersive X-ray spectroscopy
FAAS	Flame atomic absorption spectroscopy
GFAAS	Graphite furnace atomic absorption spectroscopy
ICG	Iron-coated cork granulates
ICP-OES	Inductively coupled plasma – optical emission spectrometry
OECD	Organization for Economic Co-operation and Development
pH_{PZC}	Point of zero charge
SE	Standard error
SEM	Scanning electron microscopy
S/L	Solid/liquid ratio
TDS	Total dissolved solids
TOC	Total organic carbon
WHO	World Health Organization

List of symbols

a	initial rate of adsorption (mg g^{-1} h^{-1})
a_{ya}	Yan model empirical parameter
b	coverage scale factor corresponding to the reciprocal of the coverage at which the adsorption rate has fallen to 1/e of its initial value (g mg^{-1})
BV_d	desorption bed volume
BV_b	bed volume at breakthrough
BV_s	bed volume at saturation
C	concentration of adsorbate (mg L^{-1})
C_f	final concentration of the adsorbate (mg L^{-1})
C_i	initial concentration of the adsorbate (mg L^{-1})
k_2	pseudo-second-order kinetic constant (g mg^{-1} h^{-1})
K_F	Freundlich constant (mg$^{(1-1/n)}$ L$^{1/n}$ g^{-1})
K_L	Langmuir constant (L mg^{-1})
m	mass of adsorbent (g)
m_{ad}	mass of arsenic retained in the saturated adsorbent in the previous adsorption cycle (mg)
M_d	mass of arsenic desorbed (mg)
M	mass of adsorbent in the column (g)
MTZ	mass transfer zone length (cm)
n	dimensionless parameter related to adsorbent-adsorbate affinity
p	probability of observing variation in results due to random factors
q_{ad}	adsorption capacity (mg g^{-1})
q_b	adsorption capacity at breakthrough (mg g^{-1})
q_d	desorption capacity (mg g^{-1})
q_e	adsorption capacity at equilibrium (mg g^{-1})
q_s	adsorption capacity at saturation point (mg g^{-1})
Q	flow rate (mL min^{-1})
Q_{ya}	Yan model predicted adsorption capacity (mg g^{-1})
r^2	coefficient of determination
t	time (h)
t_b	time of breakthrough (h)
t_s	saturation time (h)
T	temperature (°C)
V	solution volume (L)
V_b	breakthrough volume (L)
V_s	saturation volume (L)
y_b	arsenic removal efficiency at breakthrough (%)
y_s	arsenic removal efficiency at saturation (%)
y_d	desorption efficiency (%)

water [5,9]. Adhering to WHO guideline for arsenic in drinking water of 10 μg L^{-1} is one of the best ways to control poisoning and morbidity [10,11]. In terms of advanced water treatment technologies, adsorption is considered the most efficient and inexpensive solution [12,13], and it holds better prospects than other treatment techniques for arsenic removal [14], *e.g.* ion-exchange, phytoremediation, phytobial remediation, chemical precipitation, electrokinetic techniques, electrocoagulation, and membrane separation. Adsorption is particularly suited for places requiring systems with simple operation, little toxic sludge formation, and regeneration possibility [5]. The adsorbents can be divided into three groups: synthetic, natural, and semi-synthetic, being the last one also known as "modified biosorbents" and considered the group with the most cost-effective results [12]. Among different modification methods, iron incorporation is the most common transformation of biosorbents to increase arsenic removal rates [15].

Raw lignocellulosic biomasses have been gaining attention in recent years to produce more sustainable adsorbents [16]. Cork is a lignocellulosic natural material extracted from the bark of the cork oak tree, and it is known for its traditional usage as stopper for wine bottling [17]. Due to its high porosity and original renewable characteristic, cork has been widely studied as a biosorbent for water pollutants, including heavy metals, oils, and contaminants of emerging concern, such as pesticides, hormones, pharmaceuticals, among others [18–23]. Iron-coated cork granulates (ICG) are modified biosorbents that were developed and optimized by this research group. Characterization of the optimized material has previously been carried out through Scanning Electron Microscopy (SEM) and Electron Dispersive X-ray Spectroscopy (EDS) analysis [24]. SEM micrographs of cork granulates before and after coating revealed that the iron was deposited inside the macropores in uneven distribution, rather than as a homogeneous thin layer on the surface of the cork granulates. EDS analysis revealed iron peaks after the ferric loading. The kinetics and equilibrium of As adsorption on ICG were investigated, and distinct behavior was reported for each inorganic arsenic species [24,25], revealing a tendency for monolayer adsorption in the case of As(III) and heterogeneous multilayer adsorption for As(V). Thermodynamic studies also showed that the adsorption of arsenate onto ICG is an endothermic, spontaneous and feasible process [25].

Moreover, ICG have been successfully applied in batch operation mode for adsorption of As, Sb, and P [24,26–28] and in a continuous operation lab-scale column for removal of As [25]. Still, ICG regeneration capacity has not been yet investigated to evaluate the feasibility of the adsorbent for real application. Desorption and regeneration of any adsorbent play an important role in the adsorption process in ecological and economic terms [29]. In terms of industrial application, the regeneration over many cycles can be decisive in the choice of the adsorbent [30]. Thus, in developing a new adsorbent, it is important to study its regenerability and the desorption mechanism.

This work focuses on the desorption of arsenic from iron-coated cork granulates adsorbents in batch and continuous mode. Moreover, the regenerability of ICG was investigated, and its performance in treating real arsenic-contaminated groundwater was assessed.

2. Materials and methods

2.1. Materials

The adsorbent, iron-coated cork granulates (ICG), was produced by treating raw cork granulates (RCG) (particle size of 0.5–1.0 mm) with an iron chloride solution, in previously optimized coating conditions [24].

Arsenic aqueous solutions were diluted in distilled water from a standard solution of 1069 ± 22 mg As(V) L^{-1} or 987 ± 43 mg As(V) L^{-1}, prepared by dissolution of $HAsNa_2O_4 \cdot 7H_2O$ (Sigma-Aldrich; analytical grade) in 2 % HNO_3.

Arsenic-contaminated groundwater was prepared from a matrix of a real groundwater, collected in Northeastern Portugal. The arsenic concentration was elevated to 0.1 mg L^{-1} by spiking with an arsenic commercial standard of 1000 mg L^{-1} (Chem-Lab).

The eluent solutions were prepared by dissolving in distilled water the following chemicals: sodium hydroxide pearls 99.14 % (Labsolve), sodium carbonate anhydrous 99.5 % (Merck), nitric acid 68 % (VWR), potassium hydroxide pellets ≥85 % (Merck), potassium nitrate 99 % (Riedel-de-Haen), di-sodium ethylenediaminetetra-acetate (EDTA) > 98.5 % (May & Baker), di-sodium hydrogen phosphate dihydrate (VWR).

2.1.1. *Material characterization*

The adsorbents at different stages of saturation and regeneration were characterised by three different methodologies: acid digestion and flame atomic absorption spectroscopy (FAAS) for measuring iron content, scanning electron microscopy (SEM) for visual observation, and energy-dispersive X-ray spectroscopy (EDS) to identify the main elements present in the materials.

The methodology used in a previous study was applied for iron content determination by acid digestion [24]. In short, the materials were digested using a mixture of HCl 37 % (analytical grade, Sigma-Aldrich), HNO_3 68 % (analytical grade, VWR) and distilled water for 2 h at 150 °C. The digested solution was filtered and diluted with distilled water, and total iron content was measured by FAAS.

The SEM / EDS exam was performed using a High resolution (Schottky) Environmental Scanning Electron Microscope with X-Ray Microanalysis and Electron Backscattered Diffraction analysis: FEI Quanta 400 FEG ESEM / EDAX Genesis X4M. Samples were coated with a Au/Pd thin film by sputtering using the SPI Module Sputter Coater equipment.

2.2. *Analysis*

For column experiments and kinetics studies, total arsenic concentrations were measured by graphite furnace atomic absorption spectrometry (GFAAS) in the operating range of 6.7–50 μg L^{-1}. For batch experiments, the total arsenic concentration was measured by FAAS in the working range of 5–50 mg L^{-1} [24,26,28] and by inductively coupled plasma-optical emission spectrometry (ICP-OES) in the range of 0.005–10 mg L^{-1}. Total dissolved iron was determined by FAAS and ICP-OES in the ranges of 0.25–5.0 mg L^{-1} and 0.005–10 mg L^{-1}, respectively.

The FAAS and GFAAS equipment used in this work were a GBC 932 Plus and a GBC GF3000, respectively. The ICP-OES apparatus was an ICP-OES Thermo X Series.

The organic matter content of the aqueous solutions was quantified as total organic carbon (TOC) using a Shimadzu Equipment TOC-L.

2.3. *Batch adsorption-desorption experiments*

2.3.1. *Eluent performance*

Different eluents were selected for As(V) desorption: distilled water, NaOH (0.01 M, 0.05 M, 0.1 M, 0.5 M), Na_2CO_3 (0.01 M, 0.1 M, 0.5 M, 1 M, 2 M), HNO_3 (0.1 M), KOH (0.1 M), KNO_3 (0.5 M), EDTA (0.5 M), and Na_2HPO_4 (0.5 M). For each assay, 2.5 g L^{-1} saturated iron-coated cork granulates (3.9 ± 0.5 mg As(V) g^{-1} adsorbent) were put in contact with eluent solutions, in a rotating shaker (Stuart, SB3) at 20 rpm and a controlled temperature of 20.0 ± 0.5 °C. After 24 h of contact time, the samples were filtered using acetate cellulose filters (0.45 μm pore size) and analyzed for total As concentration by ICP-OES. The As desorbed amount (q_d, mg g^{-1}) was calculated as follows:

$$q_d = \frac{V*C}{m} \tag{1}$$

where V is the eluent solution volume (L), C is the As concentration (mg L^{-1}) desorbed to the solution, and m is the mass of saturated adsorbent (g).

The total dissolved iron was measured in the final samples after filtration to determine the extent of iron leaching from the adsorbent.

2.3.2. *Desorption kinetics*

Desorption kinetics were studied for As(V) using NaOH 0.01 and 0.1 mol L^{-1}. Like previous desorption assays, 2.5 g L^{-1} saturated iron-coated cork granulates were put in contact with the basic solution in a rotating shaker at 20 rpm and 20.0 ± 0.5 °C. The contact times were 0.25, 0.5, 1, 2, 4, 8, 16 h for NaOH 0.01 M, and 0.25, 0.5, 1, 2, 4, 8, 16 and 24 h for NaOH 0.1 M. The final solutions were filtered (acetate cellulose filters, 0.45 μm pore size) and analyzed for As by ICP-OES (assays using NaOH 0.1 M) or FAAS/GFAAS (assays using NaOH 0.01 M). The desorbed amount was calculated using Eq. (1).

2.3.3. *Adsorption-desorption cycles*

Adsorption-desorption cycles were conducted to determine the regenerability of the iron-coated cork granulates. The first cycle was always conducted with fresh ICG and the following cycles with regenerated ICG. For every cycle, an As(V) solution of 40 mg L^{-1} at pH 3.0 or a NaOH eluent solution was put in contact with ICG (S/L ratio 2.5 g L^{-1}) for a certain period in a rotating shaker at 20 rpm and a temperature of 20.0 ± 0.5 °C. Finished the experiment, the adsorbent was separated from the solution and left to dry in an oven overnight. After each desorption cycle, the adsorbent was washed for approximately 2 h to remove the residual eluent. The final solutions were filtered (acetate cellulose filters, 0.45 μm pore size) and analyzed for As by FAAS. The adsorbed amount (q_{ad}, mg g^{-1}) was calculated by mass balance (Eq. (2)), and the desorbed amount was calculated by Eq. (1).

$$q_{ad} = \frac{V\left(C_i - C_f\right)}{m} \tag{2}$$

where V is the solution volume (L), Ci and Cf are the initial and final As concentrations (mg L^{-1}), respectively, and m is the mass of adsorbent (g).

All the batch assays performed in this work were carried out in duplicate, and the result presented as the average.

2.4. *Continuous adsorption-desorption experiments*

Continuous adsorption-desorption tests were carried out in a lab-scale fixed-bed column, working in a downward flow due to the low density of the adsorbent. The lab-scale continuous adsorption system included a 50 L influent reservoir, a 30 L outlet reservoir, a glass column (Chromaflex®) with a 2.5 cm internal diameter and a maximum height of 15 cm, a peristaltic pump for flow rate regulation (VWR), an automatic sampler (GILSON, FC-203B), and a thermostatic bath for temperature control (DIGIT-COOL, J.P. SELECTA). The operational conditions were optimized in previous work and were as follows: flow rate - 5 mL min^{-1}, bed height - 12 cm, and temperature - 20 °C, which corresponds to a bed volume of 59 mL and empty bed contact time (EBCT) of 11.8 min [25]. The tests were carried out for both arsenic-spiked distilled water (1 mg As(V) L^{-1}) and arsenic-spiked groundwater (0.1 mg As L^{-1}).

The desorption assays were carried out under conditions similar to those of adsorption. The eluent applied was NaOH in concentrations of 0.1 M and 0.01 M. The desorption of arsenic from the exhausted adsorbent was conducted until arsenic concentrations in the eluent were very low. The first cycle was always conducted with fresh ICG and the following cycles with regenerated ICG.

The desorption capacity, Q_d (mg g^{-1}), was calculated as the total amount of arsenic eluted from the saturated adsorbent, divided by the total mass of adsorbent, as follows:

$$Q_d = \frac{M_d}{m} \tag{3}$$

where M_d is the As mass (mg) desorbed, and m is the mass of adsorbent (g).

The desorption efficiency (%) was calculated as the ratio between the total of arsenic eluted from the saturated adsorbent (M_d), and the mass of arsenic retained in the saturated adsorbent in the previous adsorption cycle (m_{ad}), as follows:

$$y_d = \frac{M_d}{m_{ad}} \times 100$$

2.5. Analysis of breakthrough curves

The performance of the fixed-bed column was evaluated by breakthrough curves (BTC) according to the following experimental parameters: breakthrough time (t_b), saturation time (t_s), bed volumes treated at breakthrough (BV_b), bed volumes treated at the saturation point (BV_s), adsorption capacity at breakthrough (q_b), adsorption capacity at the saturation (q_s), treated volume at breakthrough (V_b), treated volume at saturation (V_s), arsenic removal at breakthrough (y_b), arsenic removal at saturation (y_s), the mass transfer zone (MTZ) in the column, and the MTZ/Bed height ratio. The calculation of each parameter is described in a previous paper of the research group [25].

Breakthrough time was defined as that corresponding to the outlet concentration of 10 μg L^{-1}, which is the maximum level permitted in the European Union and the guideline recommended by the World Health Organization [11,31]. Theoretical parameters were obtained by fitting the Yan model to the experimental values by nonlinear regression, using *Curve Expert Pro 2.7* software. The Yan model [32] is an empirical model represented by the equation:

$$\frac{C}{C_i} = 1 - \frac{1}{1 + \left(\frac{C_i Q}{q_{Ya} * m} * t\right)^{a_{Ya}}} \tag{9}$$

Where a_{Ya} is an empirical parameter, q_{Ya} is the theoretical saturation adsorption capacity (mg g^{-1}), m is the mass of adsorbent in the column (g), C is the concentration of adsorbate at time t (mg L^{-1}), C_i is the initial adsorbate concentration (mg L^{-1}), Q is the flow rate (L min^{-1}), and t is flow time (min).

3. Results

3.1. Desorption in batch operation mode

The adsorbent's regeneration performance was firstly studied in batch operation mode. Lab-scale tests were conducted to evaluate the desorption of arsenic from ICG using several eluents, followed by the study of the effect of different eluent concentrations, and finally, the assessment of regeneration cycles by the application of consecutive adsorption-desorption cycles, using the most suitable eluent.

3.1.1. Eluent performance

The desorption of arsenate from ICG was studied by applying different classes of eluents: salts (Na_2CO_3–0.1 M and 0.5 M, Na_2HPO_4–0.5 M, KNO_3_0.5 M), bases (NaOH – 0.1 M and 0.5 M, KOH – 0.1 M), an acid (HNO_3_0.1 M), a complexing agent (EDTA – 0.5 M), and distilled water. The distilled water was able to desorb only 4.2 %. Fig. 1 and Table S.1 (Supplementary Materials) show the desorption efficiency for the other desorbing agents. The bases stood out in comparison to the salts and the acid. Among the bases, NaOH achieved the best desorption efficiencies of 83 % and 92 %, for concentrations of 0.5 M and 0.1 M, respectively, followed by KOH at 0.1 M (83 %). In the class of salts, Na_2CO_3 0.1 M achieved the best elution of 56 %. We observed that the acid option was not feasible to be applied in arsenic elution from ICG, not only because of its low desorption capacity (34 %) but also for the high extraction of iron from the adsorbent of 9.2 mg Fe g^{-1}, which was approximately 40 times higher than the iron leached in the solution using other eluents. Another iron-based sorbent for arsenic removal had also demonstrated high iron solubility from desorption using an inorganic acid eluent (638 mg L^{-1}) [33].

The overall arsenic desorption efficiency decreased in the following order: NaOH > KOH > Na_2CO_3 > HNO_3 > Na_2HPO_4 > EDTA > H_2O > KNO_3. For iron leaching from ICG, the increasing order was observed: Na_2CO_3 < H_2O < KNO_3 < Na_2HPO_4 < NaOH < KOH < EDTA < HNO_3.

The results showed that desorption efficiency was dependent on pH values (Table S.1). A pH change in solution affects both arsenate speciation and the surface charge of iron-coated cork granulates. Arsenate is prevalent in solution in the forms H_3AsO_4 (pH < 2.2), $H_2AsO_4^-$ (2.2 < pH < 6.9), $HAsO_4^{2-}$ (6.9 < pH < 11.5), and AsO_4^{3-} (pH > 11.5) [34,35], whereas the iron oxide surface is typically loaded with surface hydroxyl groups (Fe-OH), and the surface is protonated (Fe-OH_2^+) or deprotonated (Fe—O), depending on the point of zero charge (pH_{PZC}) [36]. The pH_{PZC} value for ICG is close to 6 [24], and the arsenate loading does not change this value significantly [28]. Consequently, for all pH levels of the alkaline solutions examined, the surface of ICG is deprotonated and negatively charged, resulting in the release of the negatively charged arsenate molecule [37]. A study of the "shared charge" for

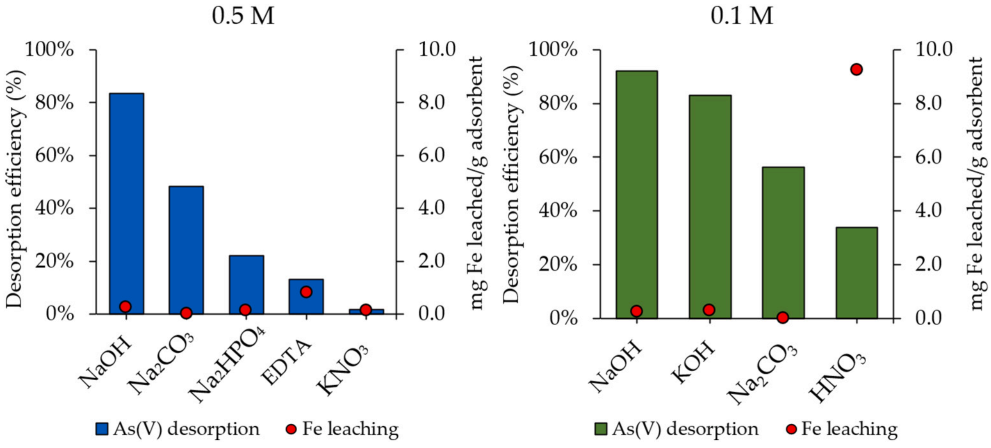

Fig. 1. Arsenate desorption efficiency and iron leaching from ICG for different eluents and concentrations (S/L ratio of 2.5 g L^{-1}; T = 20 °C).

oxyanions has found that OH^- has the highest affinity to form a bond with Fe^{3+} compared to AsO_4^{3-} and CO_3^{2-} [36], which justifies a higher desorption efficiency for NaOH and KOH solutions. However, KOH 0.1 M solution dissolved more iron than NaOH 0.1 M solution, which may have reduced its desorption efficiency.

3.1.2. Effect of eluent concentration

In this section, a deeper investigation of the effect of eluent concentration was carried out with NaOH and Na_2CO_3, which achieved the best desorption efficiency for the respective class of eluents (Section 3.1.1) and the lowest iron dissolution. The desorbing efficiency of NaOH solutions was investigated in the range 0.01–0.5 M and that of Na_2CO_3 in the range 0.01–2 M. The results are presented in Fig. 2 and Table S.1.

From Fig. 2, it can be observed that the variation in eluent concentration causes, firstly, an increase in desorption removal, followed by a decrease. The trend at higher concentrations could be caused by a degradation of the cork structure under strong basic solutions [38]. Furthermore, a similar tendency was also observed for As(V) desorption from granular ferric hydroxide (GFH) using sodium hydroxide in the range 1 % - 6 % *w/v*, with a higher desorption rate achieved for 2 % [39]. For commercial adsorbent ARM 200 (VV), the optimum NaOH concentration was found to be 4 %, with a desorption efficiency of 87.2 % [39].

The optimal concentration for both NaOH and Na_2CO_3 was found to be 0.1 M. The desorption efficiencies of basic solutions were much higher than that of salt solutions; hence, NaOH was chosen as the optimal eluent for arsenic from ICG. The iron leached from the adsorbent after 24 h in contact with 0.1 M NaOH was 0.21 mg g^{-1}, which is <1 % of the total iron content of the ICG.

The 92 % desorption efficiency of arsenate from ICG by NaOH 0.1 M was higher than that reported for other iron-based adsorbents, such as iron-impregnated biochar, with a desorbing capacity of 72 % [40], and GFH, with 36.5 % desorption, for a 1 M concentration [39].

3.1.3. Desorption kinetics

The regeneration of arsenic-loaded adsorbents can produce highly toxic waste. The minimization of both the eluent volume and chemical additions is important, and can be reached by understanding the effects of eluent composition on the equilibrium and kinetics of arsenic desorption [41]. In this section, the kinetics of As(V) desorption from ICG was investigated using NaOH 0.1 M and 0.01 M as desorbing agents. Saturated adsorbents containing 3.9 ± 0.5 mg As(V) g^{-1} and 3.7 ± 0.6 mg As(V) g^{-1} were used for assays with NaOH 0.1 M and NaOH 0.01 M, respectively. The results are presented in Fig. 3 and Table S.2.

Desorption using 0.1 M NaOH starts with a rapid increase in the first 4 h, followed by a slower second stage (4–24 h). The same trend was also observed in As(V) desorption kinetics on Ni/Mn-LDH-biochar [42] and Fe-biochar [40] in similar conditions.

The Elovich model fit to the experimental data using NaOH 0.1 M ($r^2 = 0.999$) and NaOH 0.01 M (0.978) indicates a heterogeneous surface of the adsorbent [43]. Results show a slower desorption rate for the 0.01 M NaOH solution. This decrease in desorption rate was expected given the reduction of the available molecules to cleave the arsenate bonds with the adsorbent.

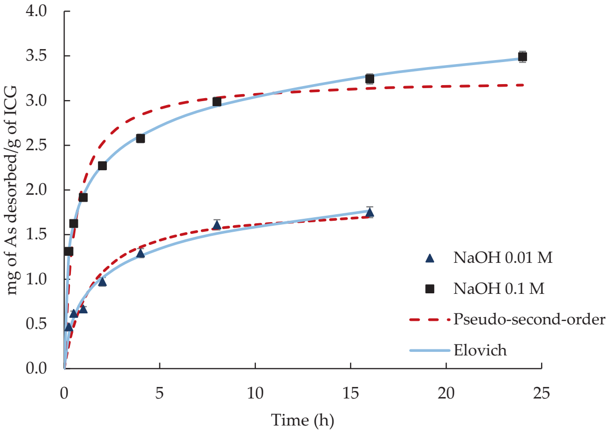

Fig. 3. Desorption kinetics for arsenate from iron-coated cork granulates using different concentrations of NaOH (20 °C; S/L = 2.5 g L^{-1}) (Error bars: standard errors).

We observed that some samples acquired an orange-yellow colouration, which could indicate a degradation of the adsorbent (Fig. S.1). So, TOC was measured to better understand the impact of eluent on the adsorbent integrity. Fig. S.2 shows that both concentrations of sodium hydroxide provoke a disintegration of the adsorbent, which leads to an increase of TOC concentration in the basic solution. The stronger basic solution caused significantly higher harm in the ICG, with higher observed TOC concentrations, especially after 4 h of contact time. The NaOH 0.01 M solution caused a steep increase in TOC after 16 contact hours. Following TOC results, desorption kinetics for NaOH 0.01 M was studied until 16 h.

At 16 h of contact, the TOC concentration in the solution was 21.4 mg L^{-1} for NaOH 0.01 M, compared to 140.7 mg L^{-1} for NaOH 0.1 M, which is approximately seven times higher. So, the NaOH 0.01 M basic solution was considered more suitable for arsenic desorption from ICG in batch mode, even leading to a lower desorbing capacity.

3.1.4. Adsorption-desorption cycles in batch operation mode

The regeneration capacity of the arsenic-loaded adsorbent was investigated in batch mode. For more insights into the effect of eluent concentration, NaOH was applied as eluent in two concentrations: 0.01 M and 0.1 M. The results of adsorption-desorption cycles are presented in Table S.3.

Even though the desorption rate with NaOH 0.01 M solution was

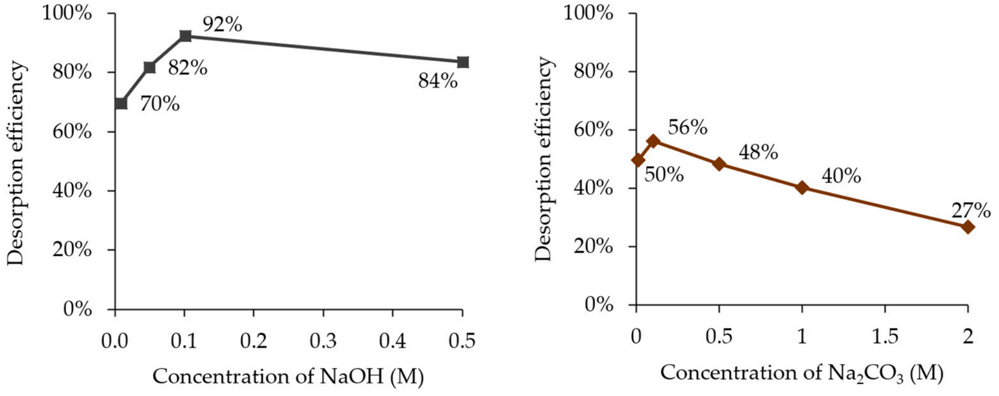

Fig. 2. Arsenate desorption efficiency using NaOH and Na_2CO_3 solutions at different concentration (S/L ratio - 2.5 g L^{-1}; *T* = 20 °C).

lower than that achieved with NaOH 0.1 M, the weaker basic eluent was able to provide better preservation of adsorption capacity in consecutive adsorption-desorption cycles. The reduction in adsorption capacity after the 1st regeneration was much higher using NaOH 0.1 M than NaOH 0.01 M. The higher TOC values obtained for the NaOH 0.1 M eluent in comparison with NaOH 0.01 M, may help justify these results (Fig. S.2). TOC represents the degradation of the adsorbent properties after contact with the desorbing agent that attacks the adsorbent structure. The loss in adsorption capacity in the successive cycles can also be related to the remaining arsenic content in the adsorbent [44]. It was evident that after highly efficient desorption, such as in the 2nd cycle, the adsorption capacity will be better maintained in the following cycle, as observed between the 2nd and 3rd cycles.

ICG was able to be regenerated by 0.01 M NaOH, for three cycles, after the first adsorption cycle using fresh ICG. The adsorbent was still able to remove high quantities of arsenic (1.0 mg g^{-1}) even after being exposed to the basic solution. The reduction in adsorption and desorption efficiency through the regeneration cycles was observed in other modified biosorbents, such as modified watermelon rind [45], iron-impregnated biochar [40], and Fe(III) modified kapok fiber [46].

3.2. Adsorption-desorption cycles in a fixed-bed column

3.2.1. Arsenic aqueous solution

Lab-scale fixed-bed column assays were conducted using 1 mg As(V) L^{-1} in distilled water for the adsorption and NaOH as eluent, in both concentrations of 0.1 M and 0.01 M, to evaluate the regeneration capacity of ICG in continuous mode. The results obtained in consecutive adsorption-desorption cycles are presented in Fig. 4 and Table S.4.

A similar trend from batch results was observed in continuous mode. The regenerated ICG presented a lower adsorption capacity in comparison to the fresh ICG, and NaOH 0.01 M could regenerate ICG for more cycles. The breakthrough curves using the regenerated ICG were very much alike, using either NaOH 0.1 M or NaOH 0.01 M.

In the first hours of adsorption with regenerated ICG, a significant concentration of arsenic in the effluent was observed, as shown in Fig. 4. However, the arsenic release decreased and ceased after a few hours, and then the typical adsorption process was initiated. The Yan model fitted well the adsorption data from all cycles ($r^2 > 0.98$).

The breakthrough time (t_b) from fresh ICG to regenerated ICG reduced from 46 to 23 h and from 46 to 25 h after treatment with NaOH 0.1 M and 0.01 M, respectively. In the following 3rd, 4th, and 5th adsorption cycles using regenerated ICG by NaOH 0.01 M t_b was 34 h, 25 h, and 16 h. Saturation time (t_s) of regenerated ICG ranged from 51 to 63 h and from 68 to 71 h, using NaOH 0.01 M and 0.1 M, respectively. The bed volumes before breakthrough ($\mathrm{BV_b}$) reduced from 253 (fresh ICG) to 147 and 140 after one desorption cycle with NaOH 0.01 M and 0.1 M, respectively. The $\mathrm{BV_b}$ decreased approximately 63 % from the 1st to the 5th adsorption cycle using NaOH 0.01 M. A reduction of about 65 % was reported from the 1st to the 4th cycle in $\mathrm{BV_b}$ of beaded coal mine drainage sludge (BCMDS-YD), using NaOH 0.1 M as desorbing agent [47].

For the adsorption cycles using NaOH 0.1 M regenerated ICG, the treated volume before breakthrough (V_b) was 14.9, 7.0, and 8.2 L. For the adsorption cycles with regeneration carried out with NaOH 0.01 M, ICG was able to treat 14.9, 8.3, 10.5, 7.7, and 5.2 L of water under 10 μg L^{-1} consecutively after desorption cycles.

Fresh ICG achieved adsorption capacities at breakthrough (q_b) and saturation (q_s) of 2.0 and 3.8 mg g^{-1} in continuous mode. The treatment by sodium hydroxide 0.01 M caused a reduction in arsenate uptake after the first regeneration cycle of 30 % and 36 % in q_b and q_s, respectively. The impact was higher when using NaOH 0.1 M, with a diminution of almost 50 % in both q_b and q_s. Fig. S.3 shows the adsorption capacities after each regeneration cycle using NaOH. The q_b of regenerated ICG decayed from 1.3 to 0.8 mg g^{-1} after four regeneration cycles using NaOH 0.01 M. For assays carried with NaOH 0.1 M, the q_b of regenerated ICG kept a constant value of 1.1 mg g^{-1}. Saturation capacities for regenerated ICG varied from 2.4 to 1.6 mg g^{-1} and from 1.9 to 2.0 mg g^{-1} using NaOH 0.01 M and 0.1 M, respectively.

The performance of breakthrough curves from fresh ICG to regenerated ICG by NaOH 0.01 M was essentially affected, with a reduction in almost all parameters (t_b, t_s, $\mathrm{BV_b}$, $\mathrm{BV_s}$, q_b, q_s, V_b, V_s, y_b, y_s) except two, MTZ and MTZ/bed height. The values of these parameters for the fixed-bed column assay using fresh ICG were 7.6 cm and 0.63, respectively, whereas for regenerated ICG using NaOH 0.01 M, they reduced to 6.9 and 0.60, 4.1 and 0.36, 6.7 and 0.58, respectively, for the 2nd, 3rd, and 4th cycles of adsorption. The shortening in these parameters means an improvement in the fixed-bed column efficiency overall by increasing the utilized bed height. The adsorption cycles using NaOH 0.1 M and the last adsorption cycle (5th) using NaOH 0.01 M presented lower fixed-bed performance, like the assay carried with fresh ICG. The fact that the fixed-bed column was more efficient through most of the adsorption cycles with regenerated ICG using NaOH 0.01 M suggests that the reduction of adsorption efficiency observed after desorption is caused by the residual arsenic content in the adsorbent.

This effect can be observed in the breakthrough curves (Fig. 4), in which BTCs after NaOH 0.01 M treatment are steeper than BTC at 1st adsorption cycle (fresh ICG) and BTCs from regeneration cycles with

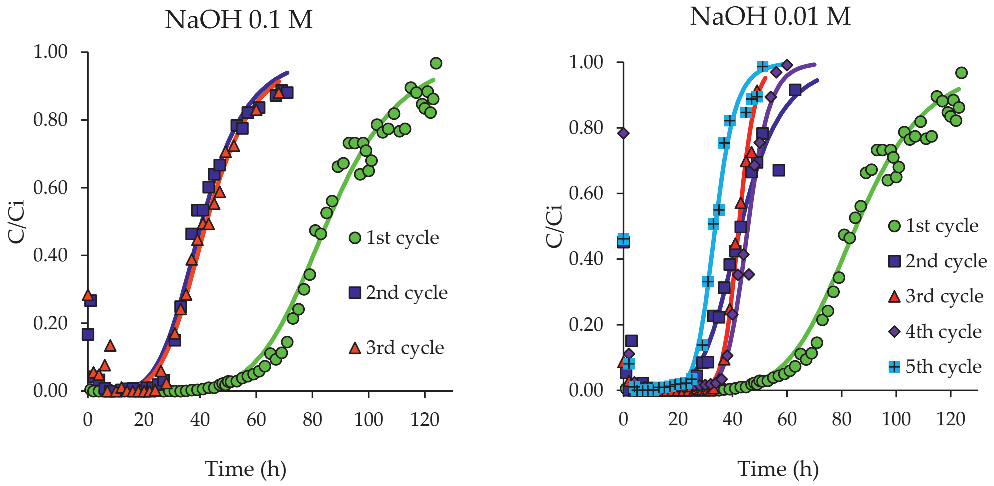

Fig. 4. Experimental (points) and predicted (lines) breakthrough curves for fresh (1st cycle) and regenerated ICG after NaOH treatment (flow rate 5 mL min^{-1} and 6 g of ICG, $C_i = 1$ mg As(V) L^{-1}, pH 3.0).

NaOH 0.1 M.

The desorption efficiency through the regeneration cycles was 62 %, 113 % and 130 % for 1st, 2nd, and 3rd desorption cycles, respectively, using NaOH 0.1 M. For the weaker basic solution, the desorption efficiencies were 74 %, 77 %, 139 %, and 103 % for the 1st, 2nd, 3rd, and 4th cycles, respectively. The desorption parameters are presented in Table S.5. The desorption capacity varied from 1.8 to 2.5 mg g^{-1} and 2.3 to 2.7 mg g^{-1} for NaOH 0.01 M and 0.1 M, respectively. The desorption capacities using the stronger basic solution were slightly higher, as observed in batch mode (item 3.1.2). The efficiencies above 100 % in some of the later desorption cycles can be explained by the desorption of residual arsenic from previous cycles.

The desorption profiles for both basic solutions are displayed in Fig. S.4. The desorption using NaOH 0.1 M was faster than NaOH 0.01 M. The stronger basic solution was able to desorb the arsenic from the adsorbent in 3 h, but the weaker base required >20 h to achieve a good desorption efficiency. This means a consumption of approximately 19 BV and 1 L of eluent using NaOH 0.1 M and about 145 BV and 8.1 L of eluent using NaOH 0.01 M. The maximum concentrations of arsenic eluted were 173.7 mg L^{-1} at 0.1 h and 30.3 mg L^{-1} at 0.5 h, for NaOH 0.1 M and 0.01 M, respectively. The maximum concentrations increased after each desorption cycle in both scenarios, suggesting that the arsenic adsorbed on the regenerated ICG was not bound as strongly to the adsorbent.

A different trend was reported in other studies where a decay in maximum concentrations of arsenic was observed after each desorption cycle [47,48]. Lee et al. (2022) reported a maximum concentration of approximately 40 mg L^{-1} of arsenic in the eluted solution after 0.2 h, 0.33 h and 0.5 h, respectively, after 1st, 2nd, and 3rd desorption cycle of saturated BCMDS, using NaOH 0.1 M. For iron-chitosan composites saturated with an inlet solution of 0.5 mg As L^{-1} the maximum concentrations of arsenic in desorption ranged from approximately 3.2 to 0.8 mg L^{-1}, using NaOH 0.1 M [48]. The highest leached arsenic concentration of roughly 25 mg L^{-1} was also observed in the first minutes of desorption of Fe-impregnated biochar using $NaHCO_3$ [49]. For sulfate-modified iron oxide-coated sand (SMIOCS), the maximum concentration of arsenic in the NaOH 0.2 M desorption solution was 5.7 mg L^{-1} after 1.5 h [50].

During regeneration cycles, the TOC and iron content in the samples were monitored. A colouration was observed in the samples after NaOH 0.1 M treatment (Fig. S.5), similarly to batch desorption (Fig. S.1). Fig. S.6 presents the boxplot graph for the TOC of samples from desorption in continuous mode. The TOC measured in the samples from each desorption cycle was on average 10.1, 11.6, 11.1, and 11.4 mg L^{-1} for 1st, 2nd, 3rd, and 4th cycles, respectively, using NaOH 0.01 M. For 1st, 2nd, and 3rd cycles of desorption using NaOH 0.1 M the average values were 109.2, 69.2, and 43.5 mg L^{-1}, respectively. The results showed a proportional increase in TOC values similar to the reported results in batch (Fig. S.2), of about 4–10 times higher concentration with NaOH 0.1 M than 0.01 M. The TOC values decayed through desorption cycles after treatment with NaOH 0.1 M, but the application of the weaker base kept TOC values almost constant through the desorption runs.

TOC results confirm the higher degradation in the ICG after treatment with NaOH 0.1 M, which justifies the limited application of the stronger basic solution for only 3 cycles in continuous mode and two cycles in batch mode (item 3.1.4). In regeneration studies conducted with iron-chitosan composites, TOC values ranging from 10.2 to 12.2 mg L^{-1} in the desorption effluent after two regeneration cycles with 0.1 M NaOH have been reported and considered to be acceptable values [48].

The adsorbent degradation can also be expressed in terms of iron leached from ICG after desorption, as the iron layer in the adsorbent is essential to keep the arsenic removal capacity in the following regeneration cycles. Fig. S.7 shows the iron leached in each desorption cycle carried out with NaOH. The maximum concentration of iron was higher for NaOH 0.1 M than for NaOH 0.01 M treatment.

The calculation of the iron leached in each assay was carried out by measuring the area below the curve of iron leaching *versus* time for each adsorption/desorption cycle. The results are presented in Table S.6. It was observed a higher iron leaching in adsorption than in desorption cycles. However, using NaOH 0.1 M, the rate of iron leaching in desorption was also high (Table S.6). This indicates that NaOH 0.1 M was more aggressive to the adsorbent than NaOH 0.01 M.

The increase in iron leaching related to an increase in NaOH concentration was also reported [41] in regeneration studies of ferric hydroxide-based adsorbents. The authors attributed the iron leaching to the formation of $Fe(OH)_2^+$ ions. The consequent decrease in the adsorbent active sites is tied to a decline in the regenerated adsorbent's performance.

The iron content was quantified in the fresh adsorbent and after 3 and 5 continuous cycles with desorption using NaOH 0.1 M and NaOH 0.01 M, respectively, to assess the degradation of the active sites in the adsorbent. Two methods were used: calculation of area below curve using experimental adsorption/desorption data and results from acid digestion of a saturated sample of adsorbent followed by FAAS (Table S.7). By calculating the iron mass balance through experimental data of iron leaching, a reduction of 19 % and 25 % of iron content (mg Fe g^{-1} ICG) was found after all adsorption-desorption cycles using NaOH 0.1 M and NaOH 0.01 M, respectively, considering the remaining iron mass and the initial adsorbent mass of 6 g. A higher reduction in iron content was expected in the material treated with NaOH 0.01 M because it went through more adsorption/desorption cycles. By acid digestion, the reduction in iron loading on regenerated ICG was 4 % and 18 %, for NaOH 0.1 M and NaOH 0.01 M, respectively (Table S.7). The difference in the iron content reduction found by each determination method can be explained by the mass loss in the cork structure, which was previously verified by TOC measurements. A more substantial mass loss is confirmed using NaOH 0.1 M due to the higher difference in the iron content values found by each method (4 % to 19 %) compared to NaOH 0.01 M (18 % to 25 %).

Fig. 5 shows SEM micrographs of fresh ICG, and ICG treated with NaOH 0.01 M and 0.1 M, in continuous mode, after 5 and 3 cycles of operation, respectively. It is possible to note that regenerated ICG have cellular structural deformation compared to fresh ICG. The ICG treated with NaOH 0.01 M (Fig. 5.b) show thinning of the cell walls but maintain the layered structure of the cells present in fresh ICG. However, the ICG treated with NaOH 0.1 M (Fig. 5.c) show further degradation, with wrinkled cells and an unstructured cellular arrangement (Fig. 5.c). Even after alkaline treatment, iron is still present in both samples in its original heterogeneous distribution, though at lower concentrations. EDS analysis of the materials is presented in Fig. S.8. The elements Fe, C, O are the most abundant in all samples and As is present in the treated samples.

Table 1 presents the effect of regeneration in different adsorbents. Generally, the adsorbent suffers a loss of adsorption capacity, which on regenerated ICG was lower than the loss suffered by iron oxide-coated biomass (IOCB) after one desorption cycle. However, other adsorbents such as commercial ArsenX^{np}, Lewatit FO36, and biosorbent rice polish could pass through desorption with a minor drop in adsorption capacity. The reduction in adsorption capacity can be related to the incomplete recovery of arsenic from the bed media or the modification in the adsorbent's properties after treatment under high pH values [41].

3.2.2. Arsenic-contaminated groundwater

Studies were conducted with natural groundwater contaminated with arsenic to evaluate the applicability of ICG in a real scenario. The groundwater characterization is shown in Table S.8.

Adsorption-desorption cycles were carried out in continuous mode using real-spiked groundwater with 0.1 mg L^{-1} of total As at the natural pH of the water of 7.09 ± 0.01. The desorption experiments were carried out with 0.1 M NaOH. The results are shown in Fig. 6, Fig. S.9 and

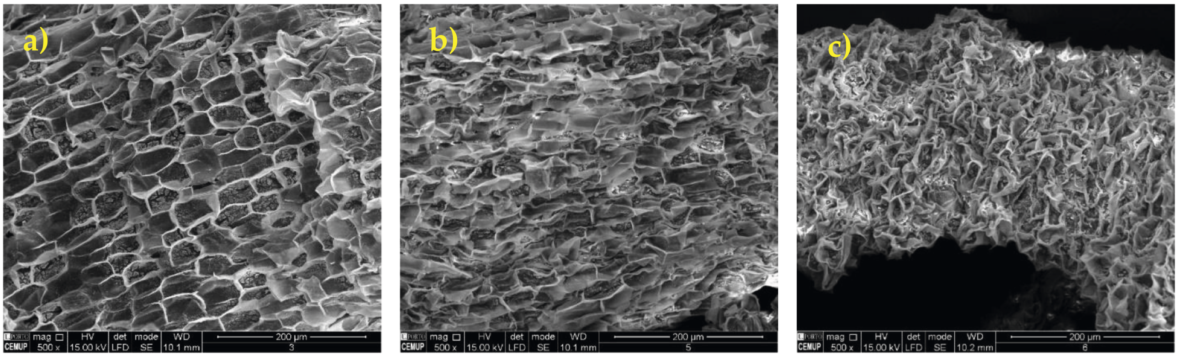

Fig. 5. SEM micrographs of: a) iron-coated cork granulates, 500× magnification, b) iron-coated cork granulates treated with NaOH 0.01 M, 500× magnification; c) iron-coated cork granulates treated with NaOH 0.1 M, 500× magnification.

Table 1
Comparison between new and regenerated adsorbents for As(V) removal in continuous mode.

Adsorbent	Cycle	Initial As concentration (μg L^{-1})	Saturation capacity (mg g^{-1})	Breakthrough time (h)	Estimated loss on adsorption capacity (%)	Ref.
Iron oxide-coated biomass (IOCB)	1st	100	0.47	–	40.4	[51]
	2nd	100	0.28	–		
ArsenX^{np}	1st	200	∼6.2	–	11.3	[52]
	2nd	200	∼5.5	–		
Lewatit FO36	1st	500	3.229	–	12.48	[53]
	2nd	500	2.826	–		
Rice polish	1st	1000	0.079	18	16.5	[54]
	2nd	1000	0.066	17		
Iron-coated cork granulates (ICG)	1st	1000	3.8	46	36.8	This study
	2nd	1000	2.4	25		

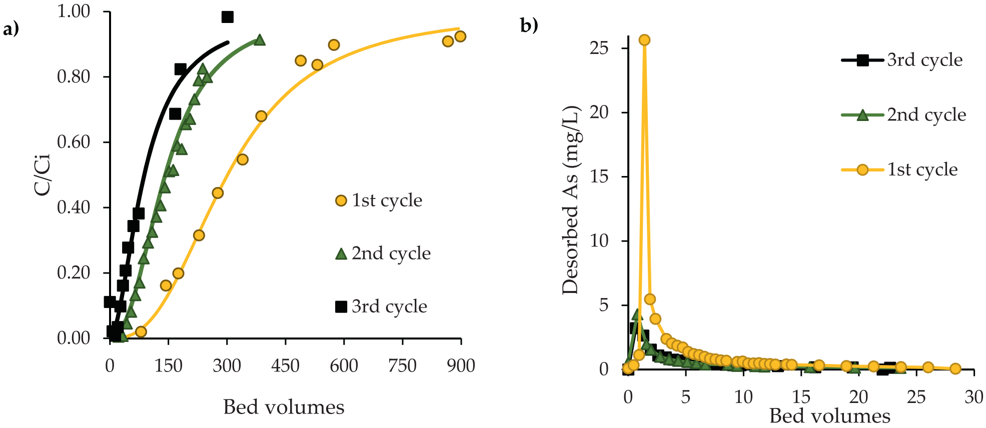

Fig. 6. Adsorption-desorption cycles: a) Experimental (points) and predicted (lines) breakthrough curves for new (1st cycle) and regenerated (2nd and 3rd cycles) ICG using real-spiked groundwater (flow rate 5 mL min^{-1} and 6 g of ICG), b) desorption profiles for three cycles using 0.1 M NaOH.

Table 2.

The breakthrough time and the arsenic removal efficiency before breakthrough (y_b) were 26 h and 99.2 %, respectively, using fresh ICG. The Yan model fitted best the breakthrough curve ($r^2 = 0.992$) with a predicted adsorption capacity of 0.26 ± 0.01 mg g^{-1}. ICG adsorption capacities from fixed-bed column studies using synthetic solutions (similar operational conditions) were reported to be 1.5 ± 0.2 mg g^{-1} for As(V) and 0.8 ± 0.1 mg g^{-1} for As(III) [25]. The reduction of arsenic adsorption capacity by ICG can be related to the presence of interferents, such as sulfates (concentration of 40.2 ± 0.2 mg L^{-1}). Sulfate was identified to reduce As(III) removal by zerovalent iron [55], zirconium-based material (ZrPACM-43) [56], and hydrous ferric oxide (HFO) [57], more specifically in the pH range from 4 to 7 [58]. The competitive effect of sulfate was also observed in As(V) adsorption by FHO [57,58], by activated modified biochar [59], and by Fe(III) modified kapok fiber [46]. The water applied in this study could either have As(V), As(III) or both species because As(III) could be already present in groundwater spiked with a general arsenic standard.

It is found in the literature that several alternative adsorbents were investigated in the removal of arsenic from real groundwater (spiked or not), as the results are shown in Table 3. It is possible to note that the adsorbents showed very similar results, with no outlier in terms of adsorption of real groundwater performance. The comparison between various adsorbents' performance is difficult because each assay was carried out in different experimental conditions, such as EBCT and initial arsenic concentration. Nevertheless, slightly better results were found in

Table 2
Experimental and predicted breakthrough parameters of arsenic adsorption from real groundwater onto fresh (first cycle) and regenerated (second and third cycle) ICG.

		Parameter	First cycle	Second cycle	Third cycle
Experimental	Breakthrough at 10 μg L^{-1}	t_b (h)	26 ± 2	10.7 ± 0.8	4.3 ± 0.6
		q_b (mg g^{-1})	0.12 ± 0.01	0.054 ± 0.004	0.025 ± 0.004
		BV_b	140 ± 13	58 ± 6	29 ± 5
		V_b (L)	7.9 ± 0.5	3.3 ± 0.3	1.6 ± 0.3
		y_b (%)	99.2 ± 0.6	98.3 ± 0.2	98.6 ± 0.3
	Breakthrough at 50 μg L^{-1}	t_b (h)	64 ± 2	27.6 ± 0.8	18.0 ± 0.8
		q_b (mg g^{-1})	0.23 ± 0.02	0.12 ± 0.01	0.09 ± 0.01
		BV_b	341 ± 25	132 ± 10	120 ± 13
		V_b (L)	19 ± 0.8	7.5 ± 0.3	6.8 ± 0.6
		y_b (%)	87 ± 1	83 ± 1	89 ± 2
	Saturation at C/C_o = ~0.90	t_s (h)	169	71	45
		q_s (mg g^{-1})	0.30 ± 0.05	0.16 ± 0.01	0.10 ± 0.09
		BV_s	898 ± 58	384 ± 25	301 ± 30
		V_s (L)	50.7 ± 0.1	21.7 ± 0.1	17.0 ± 1.4
		y_s (%)	39 ± 5	45 ± 4	39 ± 4
		MTZ (cm)	9.7	9.8	10.4
		MTZ/Bed height	0.84	0.85	0.90
Yan Model		Q_{ya} (mg g^{-1})	0.26 ± 0.01	0.14 ± 0.01	0.08 ± 0.01
		a_{ya}	2.7 ± 0.1	2.4 ± 0.1	1.8 ± 0.1
		SE (mg g^{-1})	0.03	0.03	0.04
		R^2	0.992	0.993	0.984

(± standard error of mean)

studies with iron-oxide-coated natural rock (IOCNR), iron-chitosan granules (ICB), and iron-coated cork granulates (ICG) in terms of BVs before the breakthrough.

ICG saturated with arsenic were regenerated for further adsorption tests. The results show that the adsorbent loses 50 % of its arsenic uptake capacity after each regeneration cycle but can still remove arsenic under 10 μg L^{-1} during three adsorption-desorption cycles. The adsorption rate before the breakthrough, y_b, was above 98 % in the three cycles. Nonetheless, the BV_b reduced 60 % after one regeneration cycle, from 140 to 58. This behavior was observed in other adsorbents such as iron-chitosan granules (ICB) and iron-chitosan flakes (ICF), in which regeneration by NaOH 0.1 M caused a reduction of approximately 60 % and 70 % in BV_b, respectively, for the treatment of groundwater spiked with As(V) [48].

The desorption efficiency after 1st, 2nd and 3rd cycles was 100 %, 72 % and 103.2 %, respectively. Lower desorption efficiencies were observed in commercial iron-based media such as granular ferric hydroxide (GFH) and ARM200 (LVS), treated with NaOH 1 M, of 26 % and 39 %, respectively [39]. The presence of chemical interferents such as silica was suggested as the possible cause for low arsenic desorption.

The desorption profile of each cycle (Fig. 6b) shows that maximum concentrations of arsenic eluted from the exhausted bed reduced through each cycle, from 25 to 3 mg L^{-1}. The desorption time was reduced from 6 to 3 h. In total, 2.9 L of desorption effluent was produced for the treatment of 12.8 L of groundwater under 10 μg L^{-1}. The total volume treated until the saturation point was 89.4 L.

The iron concentration in the effluent from the adsorption and desorption cycles was inferior to the EU standard in drinking water of 0.2 mg L^{-1} [31] (Fig. S.10), indicating the non-leachability of iron from the adsorbent as earlier observed at neutral pH, which is according to previous adsorption studies in continuous mode at neutral pH with ICG [25].

The results suggest that the adsorbent can be recycled in a real application. Still, better results might be obtained by a weaker base, such as 0.01 mol L^{-1} NaOH, which achieved the best regeneration performance with synthetic water in batch (item 3.1.4) and continuous mode (item 3.2.1). However, in continuous mode, the desorption using NaOH 0.01 M should take longer and produce a higher volume of waste when compared to NaOH 0.1 M. It is important to take those parameters (desorption capacity, desorption time, and volume of eluting solution) into consideration to decide which desorbing agent is more appropriate.

4. Conclusions

Desorption of arsenic from saturated iron-coated cork granulates and the performance of regenerated ICG to remove arsenic from water were investigated in this work. From batch tests it was concluded that basic solutions achieved higher desorption efficiency than salts and acid. The best desorption rate of 92 % was observed using NaOH 0.1 M. The increase in the concentration of sodium hydroxide from 0.01 M to 0.5 M showed an increase in desorption of arsenic until 0.1 M, followed by a reduction. Even though the optimum desorption efficiency in batch mode was obtained using NaOH 0.1 M, the 0.01 M concentration was less aggressive to the adsorbent and permitted ICG to be regenerated for up to four cycles with a residual adsorption capacity above 1 mg g^{-1} in both batch and continuous mode.

Total organic carbon and iron leaching were 5–10 times higher in desorption with NaOH 0.1 M than NaOH 0.01 M. The stronger degradation of ICG with NaOH 0.1 M was also confirmed by an observation of cell wall collapse in SEM micrographs. The low resistance of the structure resulted in limited performance of regenerated ICG treated with the stronger basic eluent.

Table 3
Performance of alternative adsorbents on the removal of arsenic from real (spiked) groundwater in a fixed-bed column.

Adsorbent	Bed height (cm)	EBCT (min)	Initial As concentration (μg L^{-1})	Bed volumes before the breakthrough	Breakthrough time (h)	Ref.
Iron-oxide-coated natural rock (IOCNR)	10	~3.9	40	~244	16	[60]
Laterite soil	10	~4.1	330	~100	6.75	[61]
	10	~19	179	30	~10	
Iron chitosan spacer granules (ICS)	20	~38	179	45	~29	[62]
	30	~57	179	64	~61	
XCF (xanthated chitosan flakes)	30	~57	200	99	94	[63]
Iron-chitosan granules (ICB)	30	~53	500	147	130	[48]
Iron-coated cork granulates (ICG)	12	11	100	140	26	This study

As regards adsorption and desorption capacity, the best results were achieved in continuous mode in comparison to batch mode. Adsorption capacity reduced from 3.8 ± 0.3 to 1.8 ± 0.4 mg g^{-1} from 1st to 5th adsorption cycle in continuous mode, in contrast to the reduction from 5.7 ± 0.2 to 1.0 ± 0.1 mg g^{-1} in batch mode, after NaOH 0.01 M treatment.

Fixed-bed column tests conducted with arsenic-contaminated groundwater showed the feasibility of the application of ICG in real waters, which makes it an attractive green adsorbent for commercial purposes.

This work provided good insights into arsenic desorption from ICG and the application of ICG for adsorption in real scenarios. For future work, it is important to investigate the effect of competitive elements on ICG adsorption in continuous mode, as these might be responsible for the difference in performance observed between the treatment of synthetic and natural waters.

Funding

This work was financially supported by LA/P/0045/2020 (ALiCE), UIDB/50020/2020 and UIDP/50020/2020 (LSRE-LCM), funded by national funds through FCT/MCTES (PIDDAC). A. Pintor acknowledges her Junior Researcher contract [CEECIND/01485/2017] by FCT. M. Carneiro acknowledges her Ph.D. scholarship by FCT [2020.07233.BD].

Declaration of competing interest

The authors declare that they have no known competing financial interests or personal relationships that could have appeared to influence the work reported in this paper.

Data availability

Data will be made available on request.

Acknowledgements

The authors acknowledge the Materials Center of the University of Porto (CEMUP) for SEM/EDS analyses and Eng. Liliana Pereira from the Chemical Engineering Department at the University of Porto for the ICP-OES analyses.

Appendix A. Supplementary data

Supplementary data to this article can be found online at https://doi.org/10.1016/j.jwpe.2022.103291.

References

[1] F.W. Pontius, Crafting a new arsenic rule, J. AWWA 86 (9) (1994) 6–104, https://doi.org/10.1002/j.1551-8833.1994.tb06243.x.

[2] USPHS, Public Health Service Drinking Water Standards, in: Public Health Reports (1896-1970) 58(3), 1943, pp. 69–82.

[3] O. <collab>World Health </collab>, International Standards for Drinking-water, World Health Organization, Geneva, 1958.

[4] H.-Z. Fu, M.-H. Wang, Y.-S. Ho, Mapping of drinking water research: a bibliometric analysis of research output during 1992–2011, Sci. Total Environ. 443 (2013) 757–765, https://doi.org/10.1016/j.scitotenv.2012.11.061.

[5] T.G. Asere, C.V. Stevens, G. Du Laing, Use of (modified) natural adsorbents for arsenic remediation: a review, Sci. Total Environ. 676 (2019) 706–720, https://doi.org/10.1016/j.scitotenv.2019.04.237.

[6] E. Shaji, et al., Arsenic contamination of groundwater: a global synopsis with focus on the indian peninsula, Geosci. Front. 12 (3) (2021), 101079, https://doi.org/10.1016/j.gsf.2020.08.015.

[7] R. Quansah, et al., Association of Arsenic with adverse pregnancy Outcomes/Infant mortality: a systematic review and meta-analysis, Environ. Health Perspect. 123 (5) (2015) 412–421, https://doi.org/10.1289/ehp.1307894.

[8] A. Dieudonné, et al., A sensitive magnetic arsenite-specific biosensor hosted in magnetotactic bacteria, Applied and Environmental Microbiology 86 (14) (2020), e00803-20, https://doi.org/10.1128/AEM.00803-20.

[9] S.A. Baig, et al., Arsenic removal from natural water using low cost granulated adsorbents: a review, CLEAN – soil, airWater 43 (1) (2015) 13–26, https://doi.org/10.1002/clen.201200466.

[10] A.A. Duker, E.J.M. Carranza, M. Hale, Arsenic geochemistry and health, Environ. Int. 31 (5) (2005) 631–641, https://doi.org/10.1016/j.envint.2004.10.020.

[11] Appl. Environ. Microbiol., Guidelinesfor Drinking-water Quality: Fourth Edition Incorporating First Addendum, 4th + 1st add ed., World Health Organization, Geneva, 2017.

[12] H. Patel, Fixed-bed column adsorption study: a comprehensive review, Appl Water Sci 9 (3) (2019) 1–17.

[13] S. Dudek, D. Kołodyńska, Arsenic(V) removal on the lanthanum-modified ion exchanger with quaternary ammonium groups based on iron oxide, J. Mol. Liq. 347 (2022), 117985, https://doi.org/10.1016/j.molliq.2021.117985.

[14] S. Alka, et al., Arsenic removal technologies and future trends: a mini review, J. Clean. Prod. 278 (2021), 123805, https://doi.org/10.1016/j.jclepro.2020.123805.

[15] M.A. Carneiro, et al., Current trends of arsenic adsorption in continuous mode: literature review and future perspectives, Sustainability 13 (3) (2021) 1186.

[16] L.C. Maia, L.C. Soares, L.V. Alves Gurgel, A review on the use of lignocellulosic materials for arsenic adsorption, J. Environ. Manag. 288 (2021), 112397, https://doi.org/10.1016/j.jenvman.2021.112397.

[17] A.M.A. Pintor, et al., Use of cork powder and granules for the adsorption of pollutants: a review, Water Res. 46 (10) (2012) 3152–3166, https://doi.org/10.1016/j.watres.2012.03.048.

[18] M. Mallek, et al., Granulated cork as biosorbent for the removal of phenol derivatives and emerging contaminants, J. Environ. Manag. 223 (2018) 576–585, https://doi.org/10.1016/j.jenvman.2018.06.069.

[19] V. Manzo, et al., Cork sheet as a sorptive phase to extract hormones from water by rotating-disk sorptive extraction (RDSE), Anal. Chim. Acta 1087 (2019) 1–10, https://doi.org/10.1016/j.aca.2019.08.069.

[20] T.R. de Aguiar, et al., Study of two cork species as natural biosorbents for five selected pesticides in water, Heliyon 5 (1) (2019), e01189, https://doi.org/10.1016/j.heliyon.2019.e01189.

[21] F. Krika, N. Azzouz, M.C. Ncibi, Adsorptive removal of cadmium from aqueous solution by cork biomass: equilibrium, dynamic and thermodynamic studies, Arab. J. Chem. 9 (2016) S1077–S1083, https://doi.org/10.1016/j.arabjc.2011.12.013.

[22] M. López-Mesas, et al., Bioseparation of Pb(II) and Cd(II) from aqueous solution using cork waste biomass. Modeling and optimization of the parameters of the biosorption step, Chem. Eng. J. 174 (1) (2011) 9–17, https://doi.org/10.1016/j.cej.2011.07.026.

[23] M. Crespo-Alonso, et al., Biomass against emerging pollution in wastewater: ability of cork for the removal of ofloxacin from aqueous solutions at different pH, J. Environ. Chem. Eng. 1 (4) (2013) 1199–1204.

[24] A.M.A. Pintor, et al., Arsenate and arsenite adsorption onto iron-coated cork granulates, Sci. Total Environ. 642 (2018) 1075–1089, https://doi.org/10.1016/j.scitotenv.2018.06.170.

[25] M.A. Carneiro, et al., Efficient removal of arsenic from aqueous solution by continuous adsorption onto iron-coated cork granulates, J. Hazard. Mater. (2022), 128657, https://doi.org/10.1016/j.jhazmat.2022.128657.

[26] A.M.A. Pintor, et al., Multicomponent adsorption of pentavalent as, sb and P onto iron-coated cork granulates, J. Hazard. Mater. 406 (2021), 124339, https://doi.org/10.1016/j.jhazmat.2020.124339.

[27] A.M.A. Pintor, et al., Removal of antimony from water by iron-coated cork granulates, Sep. Purif. Technol. 233 (2020), 116020, https://doi.org/10.1016/j.seppur.2019.116020.

[28] A.M.A. Pintor, et al., Complexation mechanisms in arsenic and phosphorus adsorption onto iron-coated cork granulates, J. Environ. Chem. Eng. 8 (5) (2020), 104184, https://doi.org/10.1016/j.jece.2020.104184.

[29] F. Di Natale, A. Erto, A. Lancia, Desorption of arsenic from exhaust activated carbons used for water purification, J. Hazard. Mater. 260 (2013) 451–458, https://doi.org/10.1016/j.jhazmat.2013.05.055.

[30] M. Vakili, et al., Regeneration of chitosan-based adsorbents used in heavy metal adsorption: a review, Sep. Purif. Technol. 224 (2019) 373–387, https://doi.org/10.1016/j.seppur.2019.05.040.

[31] C. <collab>European Union </collab>, in: Council Directive 2020/2184 of 16 December 2020, Off. J. Eur. Commun. L., 2020, p. 62.

[32] G. Yan, T. Viraraghavan, M. Chen, A new model for heavy metal removal in a biosorption column, Adsorpt. Sci. Technol. 19 (1) (2001) 25–43, https://doi.org/10.1260/0263617011493953.

[33] Z. Bujňáková, et al., Arsenic sorption by nanocrystalline magnetite: an example of environmentally promising interface with geosphere, J. Hazard. Mater. 262 (2013) 1204–1212, https://doi.org/10.1016/j.jhazmat.2013.03.007.

[34] M. Sadiq, T.H. Zaidi, A.A. Mian, Environmental behavior of arsenic in soils: theoretical, Water Air Soil Pollut. 20 (4) (1983) 369–377, https://doi.org/10.1007/BF00208511.

[35] G. Ungureanu, et al., Arsenic and antimony in water and wastewater: overview of removal techniques with special reference to latest advances in adsorption, J. Environ. Manag. 151 (2015) 326–342, https://doi.org/10.1016/j.jenvman.2014.12.051.

[36] T. Tuutijärvi, et al., Maghemite nanoparticles for As(V) removal: desorption characteristics and adsorbent recovery, Environ. Technol. 33 (16) (2012) 1927–1936, https://doi.org/10.1080/09593330.2011.651162.

[37] S. Sarkar, et al., Arsenic removal from groundwater and its safe containment in a rural environment: validation of a sustainable approach, Environ. Sci. Technol. 42 (12) (2008) 4268–4273, https://doi.org/10.1021/es702556t.

[38] R. Machado, J.R. Carvalho, M.Joana Neiva Correia, Removal of trivalent chromium (III) from solution by biosorption in cork powder, Journal of Chemical Technology & Biotechnology: International Research in Process, Environmental & Clean Technology 77 (12) (2002) 1340–1348.

[39] A.S.C. Chen, T.J. Sorg, L. Wang, Regeneration of iron-based adsorptive media used for removing arsenic from groundwater, Water Res. 77 (2015) 85–97, https://doi.org/10.1016/j.watres.2015.03.004.

[40] R. He, et al., Synthesis and characterization of an iron-impregnated biochar for aqueous arsenic removal, Sci. Total Environ. 612 (2018) 1177–1186, https://doi.org/10.1016/j.scitotenv.2017.09.016.

[41] B.K. Chaudhary, J. Farrell, Understanding regeneration of arsenate-loaded ferric hydroxide-based adsorbents, Environ. Eng. Sci. 32 (4) (2015) 353–360, https://doi.org/10.1089/ees.2014.0453.

[42] S. Wang, B. Gao, Y. Li, Enhanced arsenic removal by biochar modified with nickel (Ni) and manganese (Mn) oxyhydroxides, J. Ind. Eng. Chem. 37 (2016) 361–365, https://doi.org/10.1016/j.jiec.2016.03.048.

[43] K. Coenen, et al., Kinetic model for adsorption and desorption of H2O and CO2 on hydrotalcite-based adsorbents, Chem. Eng. J. 355 (2019) 520–531, https://doi.org/10.1016/j.cej.2018.08.175.

[44] S. Tresintsi, et al., A novel approach for arsenic adsorbents regeneration using MgO, J. Hazard. Mater. 265 (2014) 217–225, https://doi.org/10.1016/j.jhazmat.2013.12.003.

[45] M.B. Shakoor, et al., Arsenic removal by natural and chemically modified water melon rind in aqueous solutions and groundwater, Sci. Total Environ. 645 (2018) 1444–1455, https://doi.org/10.1016/j.scitotenv.2018.07.218.

[46] K.F.H. Yeo, et al., Adsorption performance of Fe(III) modified kapok fiber for As(V) removal from water, Sep. Purif. Technol. 287 (2022), 120494, https://doi.org/10.1016/j.seppur.2022.120494.

[47] Y. Lee, et al., Arsenic adsorption study in acid mine drainage using fixed bed column by novel beaded adsorbent, Chemosphere 291 (2022), 132894, https://doi.org/10.1016/j.chemosphere.2021.132894.

[48] A. Gupta, V.S. Chauhan, N. Sankararamakrishnan, Preparation and evaluation of iron–chitosan composites for removal of As(III) and As(V) from arsenic contaminated real life groundwater, Water Res. 43 (15) (2009) 3862–3870, https://doi.org/10.1016/j.watres.2009.05.040.

[49] X. Hu, et al., Batch and column sorption of arsenic onto iron-impregnated biochar synthesized through hydrolysis, Water Res. 68 (2015) 206–216, https://doi.org/10.1016/j.watres.2014.10.009.

[50] R.C. Vaishya, S.K. Gupta, Arsenic(V) removal by sulfate modified iron oxide-coated sand (SMIOCS) in a fixed bed column, Water Qual. Res. J. Can. 41 (2) (2006) 157–163, https://doi.org/10.2166/wqrj.2006.018.

[51] D. Pokhrel, T. Viraraghavan, Arsenic removal in an iron oxide-coated fungal biomass column: analysis of breakthrough curves, Bioresour. Technol. 99 (6) (2008) 2067–2071, https://doi.org/10.1016/j.biortech.2007.04.023.

[52] S. Sarkar, et al., Use of ArsenXnp, a hybrid anion exchanger, for arsenic removal in remote villages in the indian subcontinent, React. Funct. Polym. 67 (12) (2007) 1599–1611, https://doi.org/10.1016/j.reactfunctpolym.2007.07.047.

[53] M.R. Boldaji, et al., Evaluating the performance of iron nanoparticle resin in removing arsenate from water, J. Environ. Sci. Health A 45 (8) (2010) 946–950, https://doi.org/10.1080/10934521003772337.

[54] D. Ranjan, M. Talat, S.H. Hasan, Rice polish: an alternative to conventional adsorbents for treating arsenic bearing water by up-flow column method, Ind. Eng. Chem. Res. 48 (23) (2009) 10180–10185, https://doi.org/10.1021/ie900877p.

[55] C. Su, R.W. Puls, Arsenate and arsenite removal by zerovalent iron: effects of phosphate, silicate, carbonate, borate, sulfate, chromate, molybdate, and nitrate, relative to chloride, Environ. Sci. Technol. 35 (22) (2001) 4562–4568, https://doi.org/10.1021/es010768z.

[56] S. Mandal, M.K. Sahu, R.K. Patel, Adsorption studies of arsenic(III) removal from water by zirconium polyacrylamide hybrid material (ZrPACM-43), Water Resour. Ind. 4 (2013) 51–67, https://doi.org/10.1016/j.wri.2013.09.003.

[57] M.A. Inam, et al., Adsorption capacities of iron hydroxide for arsenate and arsenite removal from water by chemical coagulation: kinetics, thermodynamics and equilibrium studies, Molecules (Basel, Switzerland) 26 (22) (2021) 7046, https://doi.org/10.3390/molecules26227046.

[58] J.A. Wilkie, J.G. Hering, Adsorption of arsenic onto hydrous ferric oxide: effects of adsorbate/adsorbent ratios and co-occurring solutes, Colloids Surf. A Physicochem. Eng. Asp. (1996), https://doi.org/10.1016/0927-7757(95)03368-8.

[59] M.A. Alam, et al., Adsorption of as (III) and as (V) from aqueous solution by modified Cassia fistula (golden shower) biochar, Appl. Water. Sci. 8 (7) (2018) 198, https://doi.org/10.1007/s13201-018-0839-y.

[60] S.K. Maji, et al., Fixed bed adsorption of As(III) on iron-oxide-coated natural rock (IOCNR) and application to real arsenic-bearing groundwater, Chem. Eng. J. 203 (2012) 285–293, https://doi.org/10.1016/j.cej.2012.07.033.

[61] S.K. Maji, A. Pal, T. Pal, Arsenic removal from real-life groundwater by adsorption on laterite soil, J. Hazard. Mater. 151 (2) (2008) 811–820, https://doi.org/10.1016/j.jhazmat.2007.06.060.

[62] A. Gupta, N. Sankararamakrishnan, Column studies on the evaluation of novel spacer granules for the removal of arsenite and arsenate from contaminated water, Bioresour. Technol. 101 (7) (2010) 2173–2179, https://doi.org/10.1016/j.biortech.2009.11.027.

[63] A. Gupta, M. Yunus, N. Sankararamakrishnan, Equilibrium and dynamic studies of the removal of As(III) and As(V) from contaminated aqueous systems using a functionalized biopolymer, J. Chem. Technol. Biotechnol. 87 (4) (2012) 546–552, https://doi.org/10.1002/jctb.2747.